Operational calibration of a fully polarimetric radiometer for stratospheric temperature retrievals

W. Krochin, A. Murk, A. Luder, and G. Stober

Response to reviewer 2

We thank the reviewer for reading our manuscript and for providing constructive and insightful comments. We appreciate the level of detail in preparing this thorough and thoughtful review. The revised manuscript is going to be updated concerning the comments provided in the review, which improves the submitted manuscript and provides the opportunity to add more details on the instrument, calibration, and analysis scheme.

Comments on content:

- *"Title: Why include "Operational"? No operational measurements are discussed. Most critical calibration measurements are done in the lab."*

  TEMPERA-C was installed at the Jungfraujoch high-altitude observatory, where it operated continuously from March to November 2024. The crosstalk parameters c_a and c_b (as defined in Eq. 11-12) were estimated in the laboratory and were assumed to remain constant throughout the campaign. The phase shift parameter $\Delta\phi$ (defined in Eq. 40) was also initially estimated in the laboratory, but it was further operationally assessed for each measurement using the method outlined in Section 5.4. Instrument gains were calibrated operationally, utilizing an ambient load and noise diodes, with the noise diode temperatures calibrated on-site at both the beginning and the end of the campaign with an additional liquid nitrogen target. Throughout the campaign, TEMPERA-C operated without on-site maintenance. The only issues encountered were related to weather conditions and power outages at the station. The retrieved temperature time series is presented in Fig. 18.

- *"The acronym RCP can serve as an example. Despite its central importance for the final analysis, the acronym is never defined. Presumably, it means right-hand circular polarization, but there is doubt as "rc" is used for right-hand circular polarization in Eq. 6, and RCP should logically mean something else."*

  We used the acronyms "RCP" for right-hand circular polarization and "LCP" for left-hand circular polarization. The inconsistency with Eq. 6 is an unfortunate error. We will unify the notation. Thank you for highlighting this issue.

- *"Even though the calibration process is the focus of the work, the problems encountered in Sec 8 for RCP are put to the side by the comment "an artifact from the calibration process". Understandably, an issue like this can be complicated to isolate, but it should be clarified that all possible efforts have been* *made to understand the problem. Firstly, what calibration value(s) could explain the problem noticed, and what shortcoming in the setup or measurements could cause the value(s) to be wrong? Further, the radiative transfer tool used is assumed to be perfect. Presumably, modelling the Zeeman effect is a complex matter. Could there be issues in the spectroscopic parameters used, or any simplification in the implementation? Or could the information in the full Stokes vector also be analyzed for some other polarization pair (such as V and H) to shed more light on what could have gone wrong in the calibration?"*

The accuracy of the crosstalk parameters relies on the quality of the polarizing grid, the accuracy of its grid parameters, and the accuracy of the grid's rotation angle. Because the residuals in Fig. 16 and the correction term in Eq. 51 are of the same order of magnitude and similar in spectral shape (Fig. 1 in this document), we initially assumed that the residuals are caused by inaccuracies in the measurement setup mentioned above. Since in Fig. 16 only the right-circularly-polarized spectrum shows systematic residuals, spectroscopic parameters can be excluded as the cause of the error; if they were the cause, we would expect errors to be identical for both right- and left-hand circularly polarized spectra.

To further investigate the issue, we conducted a retrieval with spectra where we corrected for the complex phase offset $\Delta\phi$, but without applying the crosstalk correction (Eq. 51 and Fig. 14). The results, together with the calibrated correction term from Eq. 51, are illustrated in Fig. 1 in this document. The difference between the resulting temperature retrievals with and without the correction term remains below 0.5 K, with a maximum difference of 0.46 K. For single-polarization retrievals, the residuals are lower without using the correction term. For dual-polarization retrievals, the residuals without the correction term are lower for the right-circular but higher for the left-circular polarized spectra. This observation suggests an asymmetry between the polarizations rather than an inaccuracy in the calibration.

Recently, errors in the Zeeman algorithm of ARTS were found, primarily affecting the simulations of the linearly polarized components T_v and T_h. After consulting with the developer, we can conclude that for our observing geometry and the circularly polarized state, these errors are not significant. The asymmetry may be caused by a pathing issue, where differences in the dispersion relation lead to differences in the propagation paths of right- and left-hand-circular radiation. Since ARTS does not allow different paths for different polarizations, this asymmetry appears in the simulation. Additionally, our antenna may have a slight pointing offset between left- and right-hand circular polarizations, which could contribute to a similar effect. Since these emission lines have never been measured before, we cannot compare our measurements or simulations to other references. We will enhance our discussion by providing the analysis mentioned above. Also, we will present a comprehensive analysis of the pathing issue in our next publication.

- *"Related to the last comment above is a seeming inconsistency between different parts of the manuscript. The manuscript is about "a fully polarimetric radiometer", and the full Stokes vector is also treated in Sec. 5. However, while in Secs. 7 and 8, just two polarization states (or just the total intensity) are considered, while the full Stokes vector corresponds to four independent values. If RCP and LCP actually represent the full Stokes vector (any element zero?), this must be clarified. If this is not the case, an extended analysis, as indicated above, should be conducted."*

The instrument and its calibration is fully polarimetric. It is correct that we used just the right-hand and left-hand circular polarized spectra for the retrievals, which are only two independent Stokes components. However, a full rank Stokes vector has to be measured to obtain these spectra. The the two circular polarized states T_{lc}, T_{rc}, are calculated by $T_{lc,rc} = (T_v + T_h \pm T_4)/2$, meaning that, to calculate T_{lc}, T_{rc} all of the three components T_h, T_v, T_4 are necessary. In addition, the fourth component T_3 is necessary to estimate the crosstalk parameters c_a, c_b and the phase shift parameter $\Delta\phi$, which determines the complex rotation between T_3 and T_4 (Fig. 12). To avoid confusion, we will change the term "polarimetric retrieval" to "dual-circular-polarization retrieval"

- *"Introduction: The start of the Introduction is unclear, jumping between a broad statement about atmospheric observations and details regarding 3rd and 4th Stokes to ocean wind measurements. Consider restructuring the entire Introduction to achieve a logically flowing text. In addition, the Introduction should clarify exactly what has been done regarding full Stokes, at least within atmospheric measurements, but preferably all passive Earth observations. Some references are provided, but it is unclear whether this is a comprehensive review or merely a selection of examples."*

  We found that the applications most similar to our fully polarimetric temperature radiometer are the microwave sounders used to derive ocean wind vectors. The Special Sensor Microwave Imager/Sounder (SSMIS) on board the Air Force Defense Meteorological Satellite Program (DMSP) had 24 channels in the 60 GHz oxygen band, of which eight received right-hand circularly polarized radiation, while the others were linearly polarized (Kerola 2006, Swandley et. al. 2006, Kunkee et. al. 2008). The Microwave Limb Sounder instrument on board the Aura spacecraft observed the horizontal and vertical polarizations of the 118 GHz oxygen line (Schwartz et. al. 2011). These missions, however, did not measure the full Stokes parameters. Applications utilizing a digital correlator similar to ours have been reported in the field of radio astronomy, as proposed in Alvear et. al. 2016. For Earth observations, we were unable to find additional publications describing passive instruments that measure the full Stokes vector or their calibration. We will thoroughly revise the introduction, restructuring it and incorporating additional details along with the previously mentioned references. Also, we appreciate receiving additional references in this regard that we may have missed.

- *"Line s25-26: "The coupling to ..." Is this meant to describe the Zeeman effect? Please, describe more carefully."*

  The oxygen's magnetic dipole moment couples to the Earth's magnetic field. We will rephrase that sentence.

- *"Line 45: Not needed to also consider Doppler broadening?"*

  Doppler broadening is included in the forward model simulations using the Faddeeva function to calculate the line profile (Larsson et al., 2019). However, for the oxygen molecule at the observed frequency and altitude, pressure broadening is the dominating broadening mechanism. This is illustrated in Fig. 2 of this document, where we plot the half-width at half maximum (HWHM) over altitude for both broadening mechanisms. The figure demonstrates that even at an altitude of 60 km, the pressure broadening half-width is approximately 4 times larger than the Doppler broadening half-width.

- *"Line 47: Is this really the first investigation of this broadening? In general, there seems to be a lack of older works."*

  To our knowledge, this was the first publication reporting the Zeeman broadened shape of an oxygen fine structure emission line in the 60 GHz Band with high spectral resolution in dependence on the azimuth angle. As mentioned above, earlier studies used only a few channels in this band. The mentioned publication provides a detailed overview of the works related to Zeeman broadening theory and measurements performed within this band. We will add the most important references in our manuscript.

- *"Line 71: In what way are eight spectra obtained?*
  Lines 72-73: An incomplete sentence."

  The spectrometer is implemented in an Ettus "Universal Software Radio Peripheral" device, USRP X310, with two TwinRX daughter boards. Each of these daughter boards has two coherent input channels, which are tuned to one of the emission lines. The base-band signals are digitized with a sampling rate of 200 MS/s and 14-bit resolution, and an on-board field-programmable gate array (FPGA) performs a real-time FFT analysis. Each of the complex spectra of the two polarizations and frequency bands has a bandwidth of 100 MHz and 4096 channels. The integrator on the FPGA accumulates the total power of each linear polarization, as well as the imaginary and real parts of the cross-correlated signals. Since the two daughter boards are tuned independently to different emission lines, this results in a total of eight spectra. We will rephrase this paragraph.

- *"Line 99-101: Please explain why."*

An analogue correlator has, in general, 4 independent detectors, resulting in 4 gain parameters. Assuming that all detectors interact with each other results in 3×4= 12 additional crosstalk parameters. With 4 offset parameters, this sums up to 4+3×4+4 = 20 independent calibration parameters to estimate. Our digital correlator has two independent complex signals for input from two separate receiver chains, resulting in two complex gain parameters and two complex crosstalk parameters. After adding one offset parameter for each of the four outputs, this results in 2×2+2×2+4=12 independent real-valued calibration parameters to estimate. We expand this paragraph and provide more details in the revised manuscript to clarify these points.

- *"Line 120: "g_{33}, g_{44} are functions of g_{vv}, g_{hh}" Clarify the nomenclature. Or does this just mean that: g_{33} and g_{44} are functions of g_{vv} and g_{hh}"*

This sentence refers to the explanation above. It should express that all 16 gain parameters in Eq.6 are functions of just two complex gain parameters and two complex crosstalk parameters. We will rephrase this sentence accordingly.

- *"Line 144-145: This needs further explanation. As a general note, if any quantity is not in SI units, this needs to be clarified."*

This is a consequence of the fact that the absolute value of the complex gain has to be squared to get the same units as the elements of the gain matrix in Eq. 6. See Eq. 19 for a comparison where all elements in both matrices have the same units. We will rephrase and clarify.

- *"Line 111: What grid? It seems that a description of the measurement setup is missing. It is not sufficient to broadly refer to some references."*

An illustration of the measurement setup is shown in Fig. 9. We expand the paragraph and provide more details on the wire grid calibration experiment.

- *"Line 164: What is "principal brightness"? In any case, the meaning of T_1 and T_2 must be clarified."*

This is a misprint; it should read "principal brightness temperature." It's a corrected brightness temperature of the calibration setup after taking the grid and absorber reflectivity parameters into account. For an ideal grid and absorber with all parameters equal to zero one has, $T_1 = T_{COLD}$ and $T_2 = T_{HOT}$. We will add a further explanation in the paragraph.

- *"Equations: Please, describe more clearly how different equations are related. Eq. 39 is one such example. From what equation(s) can this be derived? For clarity, this review has not considered the details in the equations."*

Equation 39 was derived in Eq. 17-18. In general, we will expand the explanation of the equations and add more details.

- *"Line 206: T_3 and T_4 are presumably from Eq 5. However, it would be helpful to simply add (Eq. 5) after discussing T_3 and T_4."*

  We will add the reference to Eq. 5.

- *"Line 254: Here T_{LCP} and T_{RCP} are introduced. They are defined mathematically, but an explanation of their physical meaning must be added - especially their relationship to T_{lc} and T_{rc}."*

  We will unify the notation.

- *"Line 271: Isn't the azimuth angle also of importance?"*

  The Zeeman broadened lineshape in general depends on the angle between the line of sight and the magnetic field lines. This includes a dependence on the azimuth angle as well. However, for the retrieval algorithm, the Zenith angle is the key parameter since it determines the amount of air mass within the antenna beam. We will add the azimuth angle in the text.

- *"Line 283: What is a baseline correction retrieval?"*

  It's a polynomial fit added to the spectrum, where the polynomial coefficients are retrieved as part of the state vector. Usually, it's used to compensate for an instrument baseline. In this specific case, it is used to compensate for a fraction of the tropospheric contribution, which is nearly linear within the used bandwidth. The retrieved baseline is illustrated in Fig. 16.

- *"Line 286-287: "no sensor characteristics were implemented" sounds wrong. At least angles and channels are mentioned."*

  We rephrase this sentence to: "The forward model is simulated using a pencil beam and a rectangular channel response." We will also include a table that outlines the instrument specifications.

- *"Line 288: Treated as independent? In what way?"*

  This means that the noise for each channel was treated as an uncorrelated random variable with a normal distribution. We will rephrase this sentence.

- *"Line 292: Any motivation to set zc to 1 km? Later, σ_a is set to 30 K. Fluctuations of 30 K with a vertical size of about 2 km do not sound like a reasonable assumption."*

  The a priori error covariance matrix does not represent a physical situation. The fundamental assumption in the optimal estimation theory is that the physical state is normally distributed, with the a priori profile serving as the expectation value. Since the atmospheric state is not actually normally distributed, the a priori covariance is modeled to strike a balance between the smoothness of the resulting profile, convergence criteria, low cost values, and the model's flexibility to represent extreme atmospheric conditions. During the development of the retrieval algorithm, various combinations of the a priori error and correlation length were tested. Correlation lengths exceeding 1 km were found to be overly restrictive. The question of how to accurately choose the a priori covariance remains a widely debated topic within the community, with no definitive solution.

- *"Line 309: Motivate why reporting results from all these combinations? One reason is a significantly non-linear situation, but as the results throughout are similar, this does not appear to be the case."*

  Table 1-4 shows the order of magnitude in changes of the presented results depending on the choice of measurement and a priori error, and illustrates the stable convergence of the algorithm, regarding a variation of these parameters.

- *"Line 361: Presumably, the total intensity spectrum was fitted well, but please clarify."*

  Figure 1 in this document shows the residuals of the total intensity retrieval being of the same order as for the right circular spectra. We will add this illustration in the revised manuscript.

- *"Line 400-401: This refers to circular polarization, but the manuscript is about the full Stokes vector."*

  We mentioned above that our instrument operates fully polarimetric, which is necessary to obtain the two circular polarized spectra used for the retrievals. We will add this to the discussion section in our manuscript.

- *"Lines 428-429: Agreed that this improves the temporal resolution, but can this not also be achieved by other polarization pairs, such as V and H?"*

  Yes, using T_v and T_h would improve the temporal resolution by the same amount. However, the linear polarization plane has to be determined precisely. It rotates through reflections on the mirrors within the optics and would need to be estimated also in dependence of the elevation angle. This is a potential source for errors, since the Zeeman effect is very sensitive to the linear polarization plane for certain observation geometries. The advantage of circular polarization is its independence of the polarization plane. This is also the reason why we have not estimated its rotation angle or focused on the T_v,T_h or Q in this manuscript. We will add this in the discussion section.

- *"In the reply they write "Since we have never estimated the rotation of the polarization plane within the optics, our Q- and U-Stokes components are relative to a rotated polarization plane. Because of this, and because we never use the Q-Stokes component, we did not show it in the manuscript. A plot of the Q-Stokes component for this date is attached below this response." This may be clear for an expert after reading the manuscript, but it is likely to be missed by most readers."*

  We will include this in the discussion.

- *"In fact, some comments give a different impression. In the abstract, it is stated that "we present the full-rank Stokes vector". This is wrong; the Q and U components are not shown. Even if "full-rank Stokes" could be claimed to be correct in some manner, it is a misleading statement, as not all Stokes elements are determined in such a way that they can be used in the retrievals. Or any other meaningful manner?"*

  Figure 13 shows a full rank Stokes vector in the representation $\boldsymbol{T_B} = [T_v, T_h, T_3, T_4]$. In this figure, the U-Stokes component is labeled as such. However, the other labels could have led to confusion since we used a notation indexed with a, b to refer to the two receiver outputs. This was mentioned in Sec. 5.1, but should have been made clearer. We will correct this issue by unifying the notation and describing it more clearly. As mentioned above, each of the 4 Stokes components was necessary to obtain the calibrated T_{lc}, T_{rc} spectra. Related to this issue, we also considered that Fig. 1 in our manuscript could have led to confusion, since the Stokes vector there is illustrated in the representation $\boldsymbol{T_B} = [T_I, T_Q, T_U, T_V]$. We will change this figure to have the identical Stokes vector representation as used in the calibration. In addition, since it was now requested several times, we will include the panel with the Q-Stokes spectrum in the revised manuscript.

- *" To this can be added, is the simplification of the calibration only a result of the lower ambition in the determination of the Stokes elements"*

  We developed a fully polarimetric ground-based temperature radiometer to observe two Zeeman broadened emission lines on the left wing of the 60 GHz oxygen band with a high spectral resolution. The main goal are atmospheric temperature soundings with circular polarized spectra covering the altitude range of 20-60 km. We demonstrate the benefit of a dual-circular-polarized retrievals to improve the temporal resolution and altitude coverage compared to previous instruments. A crucial consideration of our developments was to sample atmospheric temperature profiles fast enough to resolve the interday variability of atmospheric solar tides. In addition, the instrument calibration had to meet the condition to allow continuous operational performance on a remote measurement site without maintenance. We demonstrated that our calibration is accurate for temperature retrievals within the specified altitude range for both total power and dual-circular-polarization retrievals. Furthermore, our results show that dual-circular-polarization retrievals have better performance. The instrument achieved a time resolution of 30 minutes and exceeds our initial goal for the time resolution, which was one hour.

- *"Is there any novelty at all in the approach?"*

  - We presented the first fully polarimetric observations of the oxygen fine structure emission lines. With 4096 channels and a spectral resolution of 25 kHz, the line shape is fully resolved for all 4 components of the Stokes Vector.
  - We performed the first temperature retrievals with two circular polarized spectra of Zeeman broadened emission lines obtained from measurements, demonstrating advantages over traditional retrieval methods.
  - We introduced the first operational fully polarimetric calibration of a temperature radiometer and we demonstrated the method within a measurement campaign.
  - Unlike existing techniques, our calibration method does not require a phase-retardation plate.
  - We developed a new case-specific approach to calibrate the complex phase shift $\Delta\phi$ by utilizing symmetry properties of the observed emission lines.
  - Our measurement site has the highest elevation recorded for a ground-based temperature radiometer to date

Technical Comments:

- *"Line 31: (Krochin et al., 2022b) The same mistake is found at other places."*

  Brackets were missed due to a formatting issue. Thank you for pointing this out.

- *"Line 54: What 7? Figure, section or equation? In addition, no need to write "see" in these references, it is implied."*

  This sentence refers to section 7. The abbreviation "Sec." wasn't shown due to a formatting issue.

- *"Figures:The descriptions of the figures are, in general, too short. Ideally, it should be possible to grasp the figure without reading the text. In general, there should not be a figure title; that information should be in the figure text. Take care of details."*

  We will revise the figure captions following these suggestions.

- *"Figure 1: As an example, write "Frequency offset [MHz]", instead of "fr offset [MHz]""*

  We will change the x axis label to "Frequency offset" in the corresponding figures.

- *"Figure 2: Explain the numbering of components in the figure text, not in the main text (neither repeat in the main text). It's a bit confusing to start the numbering of components in the first figure with 3."*

  We change the order of these figures to start the numbering at 1. Also we remove the numbering in the main text and add a legend in the figure text.

- *"Line 77: Figures shall be cited in order."*

  We will modify the order of the citations. Thank you for pointing this out.

- *"Figure 4: This figure can be removed. It does not provide any new information."*

  Figure will be removed.

- *"Figure 7: What is displayed in the second panel must be defined."*

  We will add the definition of the presented spectra.

- *"Eq 5: The mathematical notation shall distinguish between scalars, vectors and matrices. Please refer to the journal's author instructions."*

  We will correct the notation to boldface for matrices, and boldface italics for vectors.

- *"Sec 6: Most of the content of Sec 6 is found in a long series of articles, and can be removed. To leave room for describing the core content more carefully. On the other hand, some parts of Appendix A, of less standard character, are vital to understand some results. There is no reference to Appendix A, and it was first during a second reading that some details became clear."*

  We revise the appendix and link it more to the main manuscript.

- *"Line 311: There is a missing space between K, and σ_a."*

  We will ad a space there. Thank you for noting this.

- *"Line 313: Please define all acronyms. Here an explanation of MR is missing."*

  MR stands for "measurement response". Thank you for bringing this matter to our attention. We will define all acronyms in the manuscript.

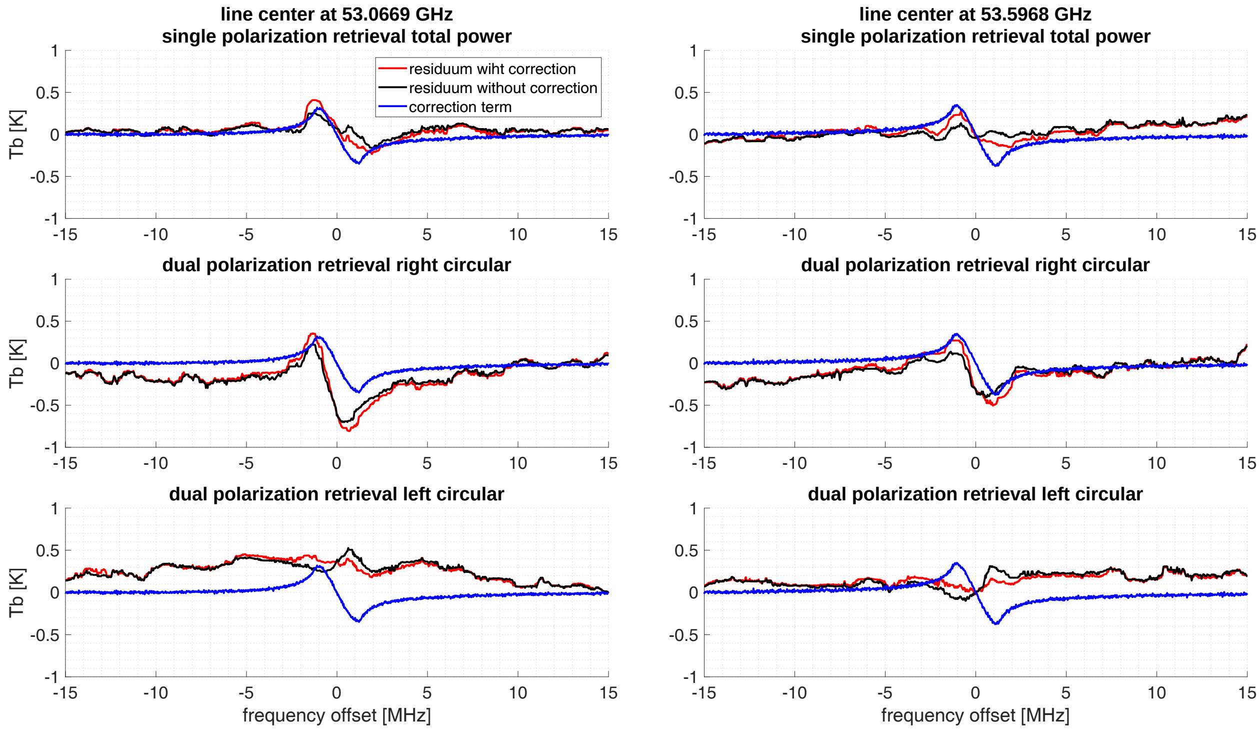

Figure 1: The residuals from the total power and dual-circular-polarization retrievals, both with and without correction for the linearly polarized components, are presented alongside the correction terms from Equation 51. The residuals have been smoothed using a moving window median with a window length of 1.2 MHz.

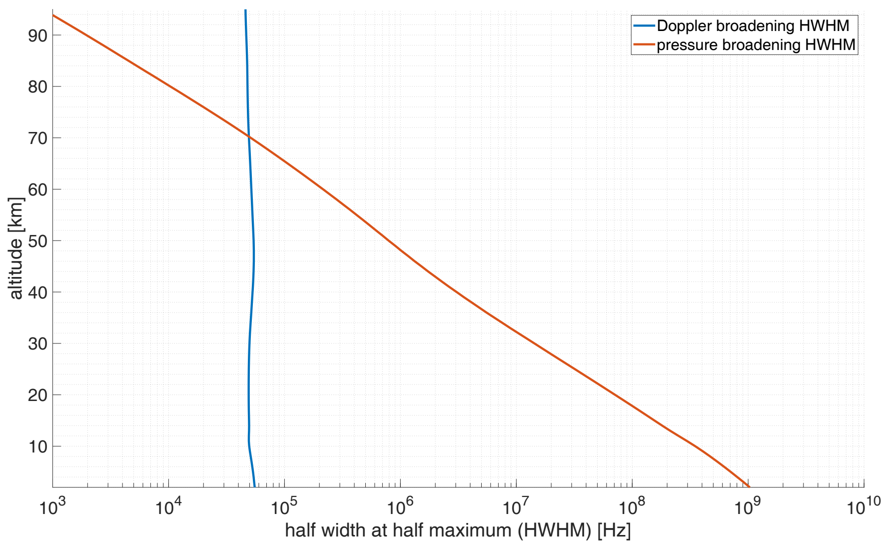

Figure 2: Doppler and pressure broadening half width at half maximum (HWHM) for O_2 and center frequency $\nu_c = 53.0669$ GHz in dependence of the altitude. Broadening parameters were taken from the HITRAN database.